RESEARCH ARTICLE

The use of fast initial response features on the homogeneously weighted moving average chart with estimated parameters under the effect of measurement errors

Maonatlala Thanwane[1] | **Saddam Akber Abbasi**[2] | **Jean-Claude Malela-Majika**[3] | **Muhammad Aslam**[4] | **Sandile Charles Shongwe**[1]

[1] Department of Statistics, College of Science, Engineering and Technology, University of South Africa, Pretoria, South Africa

[2] Department of Mathematics, Statistics & Physics, Qatar University, Doha, Qatar

[3] Department of Statistics, Faculty of Natural and Agricultural Sciences, University of Pretoria, Hatfield, South Africa

[4] Department of Statistics, Faculty of Science, King Abdulaziz University, Jeddah, Saudi Arabia

Correspondence
S.C. Shongwe, Department of Statistics, College of Science, Engineering and Technology, University of South Africa, Pretoria 0003, South Africa.
Email: sandile@tuks.co.za

Abstract

Fast initial response (FIR) features are generally used to improve the sensitivity of memory-type control charts by shrinking time-varying control limits in the earlier stage of the monitoring regime. This paper incorporates FIR features to increase the sensitivity of the homogeneously weighted moving average (HWMA) monitoring schemes with and without measurement errors under constant as well as linearly increasing variance scenarios. The robustness and the performance of the HWMA monitoring schemes are investigated in terms of numerous run-length properties assuming that the underlying process parameters are known and unknown. It is found that the FIR features improves the performance of the HWMA monitoring scheme as compared to the standard no FIR feature HWMA scheme, and at the same time, it is observed that the simultaneous use of a recently proposed FIR feature and multiple measurements significantly reduces the negative effect of measurement errors. An illustrative example on the volume of milk in bottles is used to demonstrate a real-life application.

KEYWORDS
control chart, covariate error model, fast initial response, homogenous weighted moving average, measurement error, multiple measurements

1 | INTRODUCTION

Statistical process monitoring (SPM) is the application of statistical techniques for measuring and analyzing variation in various processes to improve the quality of the products and services. The most popular statistical tool designed to serve this purpose is the control chart (or monitoring scheme). In SPM theory and practical applications, monitoring schemes are mainly used to distinguish between chance causes of variation and assignable causes of variation, as being able to distinguish between them is key to knowing whether a change that occurred resulted in either a desired or undesired end-result; see for instance, the introductory chapters in Montgomery,[1] Chakraborti and Graham,[2] and Aslam et al.[3] When only common causes of variation are present, the process is said to be in-control (IC). However, when the process has assignable causes present, it is said to be out-of-control (OOC) and corrective action to find and remove them need to

be taken. Next, when the underlying process parameters are assumed to be known, this is denoted as Case K; however, when they are assumed to be unknown, this is denoted as Case U. In the Case K scenario, monitoring can immediately be implemented to check for any departure from the IC state; however, the Case U scenario requires monitoring schemes to be applied in a two-phase approach, that is, Phase I and Phase II (see Does et al[4] for a review of recent Case U articles). Using an IC reference sample, monitoring schemes are retrospectively implemented in Phase I to estimate unknown distribution parameters. Thereafter, using the parameters estimated from Phase I, monitoring schemes are prospectively implemented in Phase II to guard against any departures from an IC state, see for instance Does et al[4] for further discussion.

Walter A. Shewhart was the first to introduce the modern monitoring scheme in the 1920s. Since then, there have been various developments such as cumulative sum (CUSUM) by Page,[5] exponentially weighted moving average (EWMA) by Roberts,[6] generally weighted moving average (GWMA) by Sheu and Lin,[7] and more recently, homogeneously weighted moving average (HWMA) by Abbas.[8] The HWMA scheme is a memory-type scheme that allocates a specific weight (equal to the smoothing parameter λ) to the current sample and distributes equally or homogenously the remaining weights (ie, equal to $1-\lambda$) to all the previous samples. The HWMA scheme is mostly considered for its effectiveness in monitoring small-to-moderate shifts in the process parameters; see also the following publications on different HWMA schemes: Adegoke et al,[9,10] Abbas et al,[11] Nawaz and Han,[12] Raza et al,[13] Adeoti and Koleoso,[14] Abid et al,[15,16] Dawod et al,[17] and Thanwane et al.[18–20] The HWMA scheme has similar limitations as the CUSUM and EWMA schemes in that it can be less sensitive in spotting start-up problems (ie, the resistance of a scheme to detect OOC samples at the beginning of the monitoring process). It is therefore a reason why this paper seeks to incorporate fast initial response (FIR) features on the HWMA scheme to enhance its responsiveness to any significant shift at the initial start-up period.

Steiner[21] studied the properties of the EWMA scheme with a basic FIR feature (denoted as BFIR). Next, Knoth[22] developed a change point model for the BFIR EWMA scheme. Chiu[23] designed a generally weighted moving average (GWMA) with a BFIR feature. Haq et al[24] proposed the modified FIR (denoted as MFIR) feature and showed that the MFIR feature has better detection ability than the Steiner's[21] BFIR feature when integrated on the EWMA and CUSUM monitoring schemes. The aforementioned researches and others concluded that FIR features shrink the time-varying control limits of the CUSUM, EWMA, and GWMA schemes, and therefore, improve their performances in detecting start-up problems. More recently, Letshedi et al[25] proposed the use of a new improved MFIR feature (denoted as IMFIR) to improve the performance of a single, double and triple EWMA schemes based on the nonparametric Wilcoxon rank-sum statistic. The IMFIR feature is shown to be more effective than the MFIR and BFIR features in detecting location shifts in a nonparametric setup. Note though, the HWMA scheme is relatively new in the literature; hence, there has not been any work on it that uses any of the abovementioned FIR features. Therefore, in this paper, the latter FIR features are applied in a parametric setup of the HWMA $\bar{X}$ scheme to improve its sensitivity during start-up period.

As per review paper by Maleki et al,[26] real-life data are mostly under the negative effect of measurement errors; which means that, a difference in magnitude between the real quantities and the measured ones mostly exist, even with highly refined innovative measuring devices. Since measurements errors are unavoidable, they need to be taken into account when monitoring items with measurements. Note that the effect of measurement errors on the performance of HWMA scheme to monitor the process mean is discussed in Thanwane et al[18,19] for Cases K and U, respectively. For some early discussions on measurement errors in SPM context, see Linna and Woodall,[27] Maravelakis et al,[28] and Maravelakis[29]; however, for some recent contributions, see Riaz et al,[30] Sabanho et al,[31,32] Zaidi et al,[33,34] Nguyen et al,[35] and Noor-ul-Amin et al.[36]

The objective of this paper is to incorporate FIR features in the time-varying control limits of the HWMA scheme to monitor the mean of processes with and without measurement errors so that its sensitivity in detecting start-up problems can be improved. In the review papers by Jensen et al,[37] Psarakis et al,[38] and Does et al,[4] it is stated that the estimation of the process parameters significantly degrades the performance of a monitoring scheme; thus, the investigation of the effect of parameter estimation on the performance of the HWMA $\bar{X}$ scheme for both a constant and linearly increasing measurement system error variances is conducted.

The rest of this paper is organized as follows: In Section 2, the proposed HWMA scheme with and without FIR features is discussed under the assumption of perfect and imperfect measurements. In Section 3, the robustness and performance of the proposed schemes are investigated in Cases K and U. Section 4 provides an illustrative example to show the application of the proposed HWMA scheme under the effect of measurement errors using the best performing FIR feature. Finally, Section 5 provides some concluding remarks.

2 | HWMA $\bar{X}$ SCHEME WITH AND WITHOUT MEASUREMENT ERRORS INTEGRATED WITH FIR FEATURES

2.1 | Phase I analysis

In Case U, Phase I analysis need to be conducted first, and thereafter, monitoring takes place in Phase II. Hence, when the process is IC, m reference samples each of size n are used to estimate the process parameters. The unbiased estimators for μ_0 and σ_0 are defined by

$$\hat{\mu}_0 = \frac{\sum_{j=1}^{m}\sum_{i=1}^{n} Y_{ji}}{mn} \tag{1}$$

and

$$\hat{\sigma}_0 = \frac{\sqrt{\frac{\sum_{j=1}^{m}\sum_{i=1}^{n}\left(Y_{ji}-\bar{Y}_j\right)^2}{m(n-1)}}}{c_{4,m}}, \tag{2}$$

respectively, where $\hat{\mu}_0$ is the IC process mean, $\hat{\sigma}_0$ is the IC process standard deviation, and $\{Y_{ji}: j = 1,\ldots,m \text{ and } i = 1,\ldots,n\}$ is a sequence of IC Phase I observations, with $\bar{Y}_j = \sum_{i=1}^{n} Y_{ji}/n$ and in Abbas[8] it is stated that the unbiasing constant is given by $c_{4,m} = \frac{\sqrt{2}\,\Gamma(\frac{m(n-1)+1}{2})}{\sqrt{m(n-1)}\,\Gamma(\frac{m(n-1)}{2})}$.

2.2 | Covariate error model for a constant and linearly increasing variance in Phase II

Let X_{ti} $\{t = 1, 2, \ldots,$ and $i = 1, 2, \ldots, n\}$ be a set of samples from Phase II of independent normal random variables such that $X_{ti} \sim N(\hat{\mu}_0 + \delta\hat{\sigma}_0,\ \hat{\sigma}_0^2)$ where $\hat{\mu}_0$ and $\hat{\sigma}_0$ represent the estimated IC mean and standard deviation, respectively, and δ denotes the magnitude of the shift in standard deviation units such that whenever $\delta = 0$, the process is said to be IC, that is, $X_{ti} \sim N(\hat{\mu}_0,\ \hat{\sigma}_0^2)$; otherwise, the process is OOC. When multiple measurements are used, an additional variable is introduced; that is, an integer $k \in \{1, 2, \ldots, r\}$, which denotes the number of measurements taken in each sampled unit.[27] Thus, the latter sequence of observations (ie, $X_{t,i}$) can only be observed through the following sequence $\{X^*_{t,i,k} : t = 1,2,\ldots;$ $i = 1,2,\ldots, n;\ k = 1,\ldots, r\}$. Each value in the sequence is calculated by

$$X^*_{t,i,k} = A + BX_{t,i} + \varepsilon_{t,i,k}, \tag{3}$$

where $\varepsilon_{t,i,k} \sim N(0, \sigma_M^2)$ is a random error due to measurement error and it is distributed independently of $X_{t,i}$.[26] Note that σ_M^2 is the variance of the measurement system. Moreover, the two constants, A and B in Equation (3), depend on the measurement system location error.[27] In addition, according to Linna and Woodall[27] when the measurement system error variance is assumed to be constant, it follows that

$$X^*_{t,i,k} \sim N\left(A + B\hat{\mu}_0,\ B^2\hat{\sigma}_0^2 + \sigma_M^2\right). \tag{4}$$

However, in some of the real-life applications, the measurement system error variance, σ_M^2 is an increasing function of the mean of the variable $X_{t,i}$, that is, $\sigma_M^2 = C + D\hat{\mu}_0$, where C and D are two constants depending on the measurement system variability error. Hence, Linna and Woodall[27] showed that in the case of the corresponding linearly increasing error variance, Equation (4) becomes

$$X^*_{t,i,k} \sim N\left(A + B\hat{\mu}_0,\ B^2\hat{\sigma}_0^2 + D\hat{\mu}_0\right). \tag{5}$$

Thus, the mean of n observations from the sequence $X^*_{t,i,k}$ at each sampling point is defined by

$$\bar{X}^*_t = \frac{1}{nr}\sum_{i=1}^{n}\sum_{k=1}^{r} X^*_{t,i,k} = A + B\frac{1}{n}\sum_{i=1}^{n} X_{t,i} + \frac{1}{nr}\sum_{i=1}^{n}\sum_{k=1}^{r}\varepsilon_{t,i,k}. \tag{6}$$

Note that

$$E\left(\bar{X}^*_t\right) = A + B\frac{1}{n}\sum_{i=1}^{n} E\left(X_{t,i}\right) + \frac{1}{nr}\sum_{i=1}^{n}\sum_{k=1}^{r} E\left(\varepsilon_{t,i,k}\right) = A + B\hat{\mu}_0. \tag{7a}$$

Next,

$$\begin{aligned}
\mathrm{Var}\left(\bar{X}^*_t\right) &= \mathrm{Var}\left(A\right) + \mathrm{Var}\left(B\frac{1}{n}\sum_{i=1}^{n} X_{t,i}\right) + \mathrm{Var}\left(\frac{1}{nr}\sum_{i=1}^{n}\sum_{k=1}^{r}\varepsilon_{t,i,k}\right)\\
&= B^2\frac{1}{n^2}\mathrm{Var}\left(\sum_{i=1}^{n} X_{t,i}\right) + \frac{1}{(nr)^2}\sum_{i=1}^{n}\sum_{k=1}^{r}\mathrm{Var}\left(\varepsilon_{t,i,k}\right)\\
&= B^2\frac{1}{n^2}\left(\sum_{i=1}^{n}\mathrm{Var}\left(X_{t,i}\right) + 2\sum_{t<\upsilon}\sum\mathrm{Cov}\left(X_{t,i},X_{\upsilon,i}\right)\right)\\
&\quad + \frac{1}{(nr)^2}\left(\sum_{i=1}^{n}\sum_{k=1}^{r}\mathrm{Var}\left(\varepsilon_{t,i,k}\right) + 2\sum_{t<\upsilon}\sum\sum\sum\mathrm{Cov}\left(\varepsilon_{t,i,k},\varepsilon_{t,i,k}\right)\right).
\end{aligned}$$

Since the sequence $\{X_{t,i}\}$ is i.i.d., it follows that $\mathrm{Cov}\left(X_{t,i},X_{\upsilon,i}\right) = 0$ for any $t \neq \upsilon$ and $\mathrm{Var}\left(X_{t,i}\right) = \hat{\sigma}_0^2$. Similarly, $\mathrm{Cov}\left(\varepsilon_{t,i,k},\varepsilon_{\upsilon,i,k}\right) = 0$ and $\mathrm{Var}\left(\varepsilon_{t,i,k}\right) = \sigma_M^2$. Thus, it follows that

$$\mathrm{Var}\left(\bar{X}^*_t\right) = \frac{B^2\hat{\sigma}_0^2}{n} + \frac{\sigma_M^2}{nr} = \frac{rB^2\hat{\sigma}_0^2 + \sigma_M^2}{nr}. \tag{7b}$$

2.3 | HWMA scheme with measurement errors

The HWMA $\bar{X}^*$ scheme under the negative effect of measurement errors in Case U were discussed in Thanwane et al[19] and its plotting statistic is given by

$$H^*_t = \lambda\bar{X}^*_t + (1-\lambda)\overline{\overline{X}}^*_{t-1}, \tag{8}$$

where $\bar{X}^*_t$ is given in Equation (6), $\overline{\overline{X}}^*_{t-1}$ is the mean of the previous t–1 sample means computed by

$$\overline{\overline{X}}^*_{t-1} = \frac{1}{t-1}\sum_{l=1}^{t-1}\bar{X}^*_l,$$

The initial value of $\overline{\overline{X}}^*_0$ (at $t = 1$, ie, $\overline{\overline{X}}^*_0$) is set to be equal to the target mean $A + B\hat{\mu}_0$ in Equation (7a) and its variance is given by

$$Var\left(\overline{\overline{X}}^*_0\right) = Var\left(A + B\hat{\mu}_0\right) = 0. \tag{9}$$

Thus, using Equation (7a), it follows that the expected value of H_t^* is given by

$$E\left(H_t^*\right) = \lambda E\left(\bar{X}_t^*\right) + (1-\lambda)E\left(\bar{\bar{X}}_{t-1}^*\right) = A + B\hat{\mu}_0. \tag{10}$$

The variance of Equation (8) is calculated in two parts, that is, $t = 1$ and $t > 1$. That is, using Equations (7b) and (9), it follows that at $t = 1$,

$$\text{Var}\left(H_1^*\right) = \sigma^2_{H_1^*} = \lambda^2\,\text{Var}\left(\bar{X}_1^*\right) + (1-\lambda)^2\text{Var}\left(\bar{\bar{X}}_0^*\right) = \lambda^2\frac{rB^2\hat{\sigma}_0^2 + \sigma_M^2}{nr}.$$

However, since the observations are i.i.d. and using Equation (7b),

$$\text{Var}\left(\bar{\bar{X}}_{t-1}^*\right) = \text{Var}\left(\frac{1}{t-1}\sum_{l=1}^{t-1}\bar{X}_l^*\right) = \frac{1}{(t-1)^2}\sum_{l=1}^{t-1}\text{Var}\left(\bar{X}_l^*\right) = \frac{1}{t-1}\left(\frac{rB^2\hat{\sigma}_0^2 + \sigma_M^2}{nr}\right)$$

and thus, it follows that at $t > 1$,

$$\text{Var}\left(H_t^*\right) = \sigma^2_{H_t^*} = \lambda^2\text{Var}\left(\bar{X}_t^*\right) + (1-\lambda)^2\text{Var}\left(\bar{\bar{X}}_{t-1}^*\right) = \lambda^2\left(\frac{rB^2\hat{\sigma}_0^2 + \sigma_M^2}{nr}\right) + (1-\lambda)^2\frac{1}{t-1}\left(\frac{rB^2\hat{\sigma}_0^2 + \sigma_M^2}{nr}\right).$$

Stated differently,

$$\text{Var}\left(H_t^*\right) = \sigma^2_{H_t^*} = \begin{cases} \lambda^2\dfrac{rB^2\hat{\sigma}_0^2 + \sigma_M^2}{nr}, & t = 1 \\ \left(\lambda^2 + \dfrac{(1-\lambda)^2}{t-1}\right)\dfrac{rB^2\hat{\sigma}_0^2 + \sigma_M^2}{nr}, & t > 1. \end{cases} \tag{11}$$

The time-varying control limits of the HWMA $\bar{X}^*$ scheme with a constant measurement system variance and r-measurements are defined by:

$$UCL_t/LC\,L_t = \begin{cases} (A + B\hat{\mu}_0) \pm L^*\sqrt{\dfrac{\lambda^2\hat{\sigma}_0^2}{n}\left(\dfrac{rB^2 + \gamma^2}{r}\right)}, & t = 1 \\ (A + B\hat{\mu}_0) \pm L^*\sqrt{\left(\dfrac{\lambda^2\hat{\sigma}_0^2}{n} + \dfrac{(1-\lambda)^2\hat{\sigma}_0^2}{n(t-1)}\right)\left(\frac{rB^2+\gamma^2}{r}\right)}, & t > 1, \end{cases} \tag{12a}$$

where L^* is a control limit coefficient of the HWMA $\bar{X}^*$ scheme and $\gamma = \frac{\sigma_M}{\hat{\sigma}_0}$ denotes the standardized ratio of the variabilities of the measurement system to that of the process one. However, the time-varying control limits of the HWMA $\bar{X}^*$ scheme with a linearly increasing variance and r-measurements are defined by

$$UCL_t/LC\,L_t = \begin{cases} (A + B\hat{\mu}_0) \pm L^*\sqrt{\lambda^2\left(\dfrac{rB^2\hat{\sigma}_0^2 + C + D\hat{\mu}_0}{nr}\right)}, & t = 1 \\ (A + B\hat{\mu}_0) \pm L^*\sqrt{\left(\lambda^2 + \dfrac{(1-\lambda)^2}{t-1}\right)\left(\dfrac{rB^2\hat{\sigma}_0^2 + C + D\hat{\mu}_0}{nr}\right)}, & t > 1. \end{cases} \tag{12b}$$

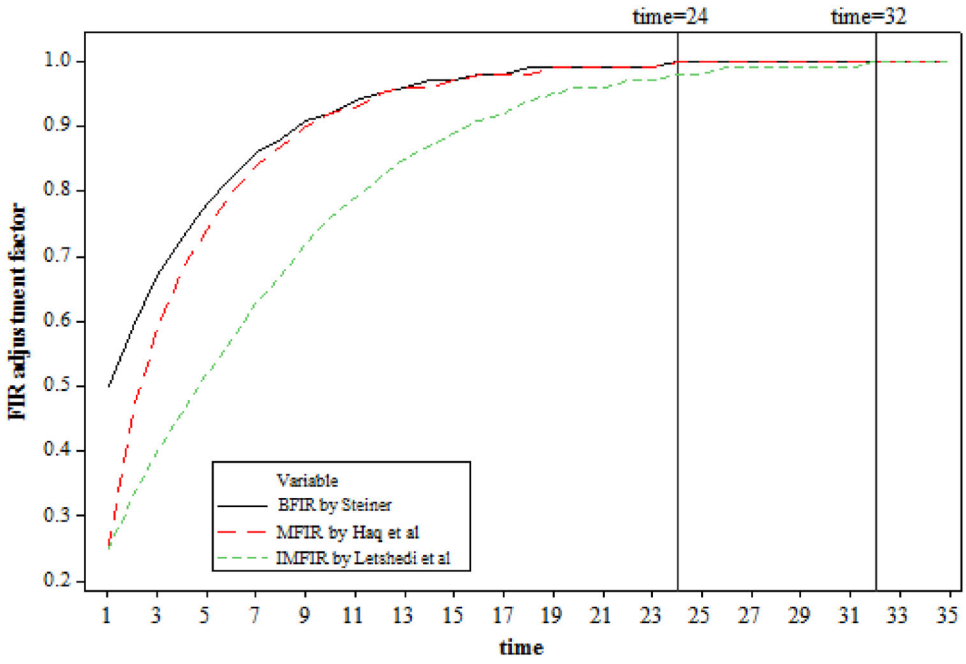

FIGURE 1 Comparison of the BFIR, MFIR, and IMFIR adjustment features with respect to the time t

Note that the HWMA $\bar{X}^*$ scheme without measurement errors is designed in similar way; however, assuming that $\gamma = \frac{\sigma_M}{\hat{\sigma}_0} = 0$ or $\sigma_M^2 = C + D\hat{\mu}_0 = 0$ and $r = 1$.

2.4 | HWMA monitoring scheme with FIR features

Mostly known to some authors as a "head-start," a FIR feature enhances the sensitivity of the monitoring schemes during start-up period. This feature improves the performance of a scheme at a start-up or after an OOC signal. FIR features may be implemented when a practitioner suspects there is a possibility of very small shift or wants to guard against possible small or large shifts during start-up period.[39] Initial response features considered here are a power transformation adjustment factor (denoted as FIR_{adj}) such that when the effect of FIR has completely disappeared, the FIR_{adj} equals 1. According to Steiner,[21] Haq et al,[24] and Letshedi et al,[25] the BFIR, MFIR, and IMFIR features are respectively given by

$$\text{BFIR}_{\text{adj}} = 1 - (1-f)^{1+a(t-1)}, \tag{13a}$$

$$\text{MFIR}_{\text{adj}} = \left\{1 - (1-f)^{1+a(t-1)}\right\}^{1+\frac{1}{t}}, \tag{13b}$$

$$\text{IMFIR}_{\text{adj}} = \left\{1 - (1-f)^{1+a(t-1)}\right\}^{\sqrt{t}\left(1+\frac{1}{t}\right)}, \tag{13c}$$

where f denotes a segment of an interval from a start-up value to the control limits, where a and f were suggested to be equal to 0.3 and 0.5, respectively.

Using $a = 0.3$, $f = 0.5$, and $t \geq 1$, it is observed in Figure 1 that the $\text{IMFIR}_{\text{adj}}$ has the lowest magnitude as compared to MFIR_{adj} (second lowest) and BFIR_{adj} (highest). The MFIR_{adj} is smaller than the BFIR_{adj} when $t < 19$ (see also Haq et al[24]) and converges to 1 at $t \geq 24$. However, the $\text{IMFIR}_{\text{adj}}$ is smaller than the BFIR_{adj} and MFIR_{adj} when $t < 32$ (see also Letshedi et al[25]) and from $t \geq 32$, all the FIR features are exactly equal to 1. While the effect of FIR features disappears as time increases, it is important to note that for the standard "no FIR" scenario, the FIR_{adj} is equal to 1 for all values of t.

Incorporating Equations (13a) to (13c) into Equations (12a) and (12b), then it follows that the control limits of the HWMA scheme with FIR_{adj} for the constant measurement system variance is given by

$$UCL_t/LC\ L_t = \begin{cases} (A + B\hat{\mu}_0) \pm \text{FIR}_{\text{adj}} L^* \sqrt{\dfrac{\lambda^2\hat{\sigma}_0^2}{n}\left(\dfrac{rB^2+\gamma^2}{r}\right)}, & t = 1 \\ (A + B\hat{\mu}_0) \pm \text{FIR}_{\text{adj}} L^* \sqrt{\left(\dfrac{\lambda^2\hat{\sigma}_0^2}{n} + \dfrac{(1-\lambda)^2\hat{\sigma}_0^2}{n(t-1)}\right)\left(\dfrac{rB^2+\gamma^2}{r}\right)}, & t > 1; \end{cases} \tag{14a}$$

however, for the linearly increasing measurement system variance, the control limits are given by

$$UCL_t/LCL_t = \begin{cases} (A + B\hat{\mu}_0) \pm \text{FIR}_{\text{adj}} L^* \sqrt{\lambda^2\left(\dfrac{rB^2\hat{\sigma}_0^2 + C + D\hat{\mu}_0}{nr}\right)}, & t = 1 \\ (A + B\hat{\mu}_0) \pm \text{FIR}_{\text{adj}} L^* \sqrt{\left(\lambda^2 + \dfrac{(1-\lambda)^2}{t-1}\right)\left(\dfrac{rB^2\hat{\sigma}_0^2 + C + D\hat{\mu}_0}{nr}\right)}, & t > 1, \end{cases} \tag{14b}$$

where FIR_{adj} denotes the BFIR_{adj}, MFIR_{adj}, and $\text{IMFIR}_{\text{adj}}$ given in Equations (13a), (13b), and (13c), respectively.

Note that the HWMA $\bar{X}^*$ scheme integrated with BFIR, MFIR, and IMFIR features are denoted as BFIR-HWMA, MFIR-HWMA, and IMFIR-HWMA, respectively. Hence, the BFIR-HWMA, MFIR-HWMA, and IMFIR-HWMA schemes with the constant and linearly increasing variances give a signal when the plotting statistic defined in Equation (8) plots beyond the control limits defined in Equations (14a) and (14b), respectively.

3 | PERFORMANCE OF HWMA $\bar{X}^*$ SCHEME WITH AND WITHOUT FIR FEATURES

3.1 | Performance metrics

To investigate the sensitivity of a monitoring scheme, the characteristics of the run-length (*RL*) distribution are often used. The *RL* represents the number of charting statistics to be plotted on the scheme before the first OOC signal. The expected *RL*, that is, average *RL* (*ARL*), is the most used performance metric when the operator is interested to assess the performance of a scheme for a specific shift (δ). The *ARL* can be computed using exact formulas,[27] Markov chain technique,[39] or Monte Carlo simulation.[24] In this paper, Monte Carlo simulations with 50 000 replications were implemented in SAS® v9.4 software to compute the *RL* properties of the proposed HWMA $\bar{X}^*$ scheme with and without FIR features. Other popular *RL* properties that are used to evaluate the performance of a monitoring scheme are the standard deviation of the *RL* (*SDRL*) as well as the percentiles run-length (*PRL*), that is, 5th, 25th, 50th, 75th, and 95th percentiles (denoted as P5, P25, P50, P75, and P95), respectively.

When the operator is interested to assess the performance of a scheme for a range of shifts, the expected *ARL* (*EARL*) is usually preferred.[40,41] In this paper, the *EARL* metric is used to investigate the overall performance of the proposed schemes for a range of shifts and it is defined by the following Riemann sum:

$$EARL_{(\delta_{\min},\delta_{\max}]} = \frac{1}{\Delta}\sum_{\delta=\delta_{\min}}^{\delta_{\max}} ARL(\delta), \tag{15}$$

where $\delta_{\min} = 0$ (lower limit of δ, not included in the summation) and $\delta_{\max} = 1$ (upper limit of δ) and $\Delta = 10$ represents the number of increments between $\delta_{\min}$ and $\delta_{\max}$.

TABLE 1 IC ARL and SDRL profiles of the HWMA $\bar{X}^*$ scheme with and without FIR features when $m = 100$, $n = 5$, and $\lambda = 0.1$ under different continuous probability distributions with a nominal $ARL_0 = 500$

	IC *ARL*				IC *SDRL*			
	None	**BFIR**	**MFIR**	**IMFIR**	**None**	**BFIR**	**MFIR**	**IMFIR**
$N(0,1)$	500.5	501.9	501.6	505.9	569.3	804.3	1082.1	1262.4
$t(5)$	234.3	208.3	159.0	142.3	205.3	247.3	270.9	279.9
$t(10)$	365.7	349.2	310.4	300.9	369.2	457.5	595.6	649.3
$t(20)$	436.0	434.3	404.2	393.0	476.2	607.4	837.3	917.2
GAM(1, 1)	292.4	244.2	175.1	147.4	354.6	385.6	416.7	381.4
GAM(3, 1)	409.4	383.6	326.4	312.5	485.0	589.1	777.7	875.3
GAM(10, 1)	466.1	468.1	438.6	438.0	540.3	706.2	979.8	1161.7

3.2 | Robustness study

A monitoring scheme is said to be IC robust when the characteristics of the IC *RL* are approximately the same or much closer across all continuous probability distributions; see Chakraborti and Graham[2] for more details on this concept. To evaluate whether the HWMA $\bar{X}^*$ scheme with and without FIR features is robust, the standard normal distribution (denoted by $N(0,1)$), Student's t distribution (denoted by $t(\nu)$) and the Gamma distribution (denoted by $GAM(\omega, \beta)$) are considered. For the $t(\nu)$ distribution, the degrees of freedom considered are $\nu = 5, 15, 30$; however, for the $GAM(\omega, \beta)$ distribution, the location, and scale parameters considered are $\omega = 1, 3, 10$ and $\beta = 1$, respectively. More importantly, the latter distributions with different parameters are each transformed such that the mean and standard deviation are equal to 0 and 1, respectively.

In general, it is observed from Table 1 that the values of the IC *ARL* and *SDRL* values are not approximately the same for different underlying distributions and thus, each of the four monitoring schemes are not IC robust. Stated differently, the HWMA $\bar{X}^*$ scheme with and without the FIR features are not IC robust, for any level of measurement error, since the *RL* properties (ie, the IC *ARL* and *SDRL*) are not approximately equal across different distributions. Note that, while the process is IC, the *SDRL* of the HWMA schemes with FIRs are generally larger than that of the "no FIR" one. While this is shown for $m = 100$, it also holds for other Phase I sample sizes. Furthermore, in Figure 2, it is shown that the *PRL* characteristics are not approximately equal (or form a horizontal plot) across the different distributions in both Cases K and U (with the exception of the P5, P25, and P50 in some few instances). Note that, although not shown here, it is worth mentioning that similar patterns as those in Table 1 and Figure 2 are also observed for different Phase I and Phase II sample sizes as well as different ARL_0 values.

3.3 | Sensitivity analysis

3.3.1 | HWMA $\bar{X}^*$ scheme for different FIR features with no measurement errors

Note that increasing values of the *ARL* and *EARL* are indicative of a deteriorating process; however, decreasing values are indicative of an improving process. For the HWMA $\bar{X}^*$ scheme without measurement errors, the effect of integrating FIR feature on the HWMA scheme is illustrated in Table 2 for Cases K and U. It is observed that the *ARL*s are higher in Case U as compared to Case K for each corresponding HWMA $\bar{X}^*$ scheme with a FIR feature; this indicates that the Phase I estimation has a negative effect on the Phase II performance. More importantly, for a specific value of m, the magnitude of the *ARL* (for each shift) and *EARL* (over range of shifts), it is observed that the HWMA $\bar{X}^*$ schemes can be sorted as follows, in both Cases K and U:

$$\text{HWMA} > \text{BFIR} - \text{HWMA} > \text{MFIR} - \text{HWMA} > \text{IMFIR} - \text{HWMA}. \tag{16}$$

According to Table 3, when parameters are estimated from Phase I, the HWMA scheme with "no FIR" has the worst *SDRL* especially when m is small; however, in Case K, it has the best OOC *SDRL* performance as compared to the HWMA scheme with FIR features. Moreover, the relation in Equation (16) for the *SDRL* only holds in Case U scenario; not in

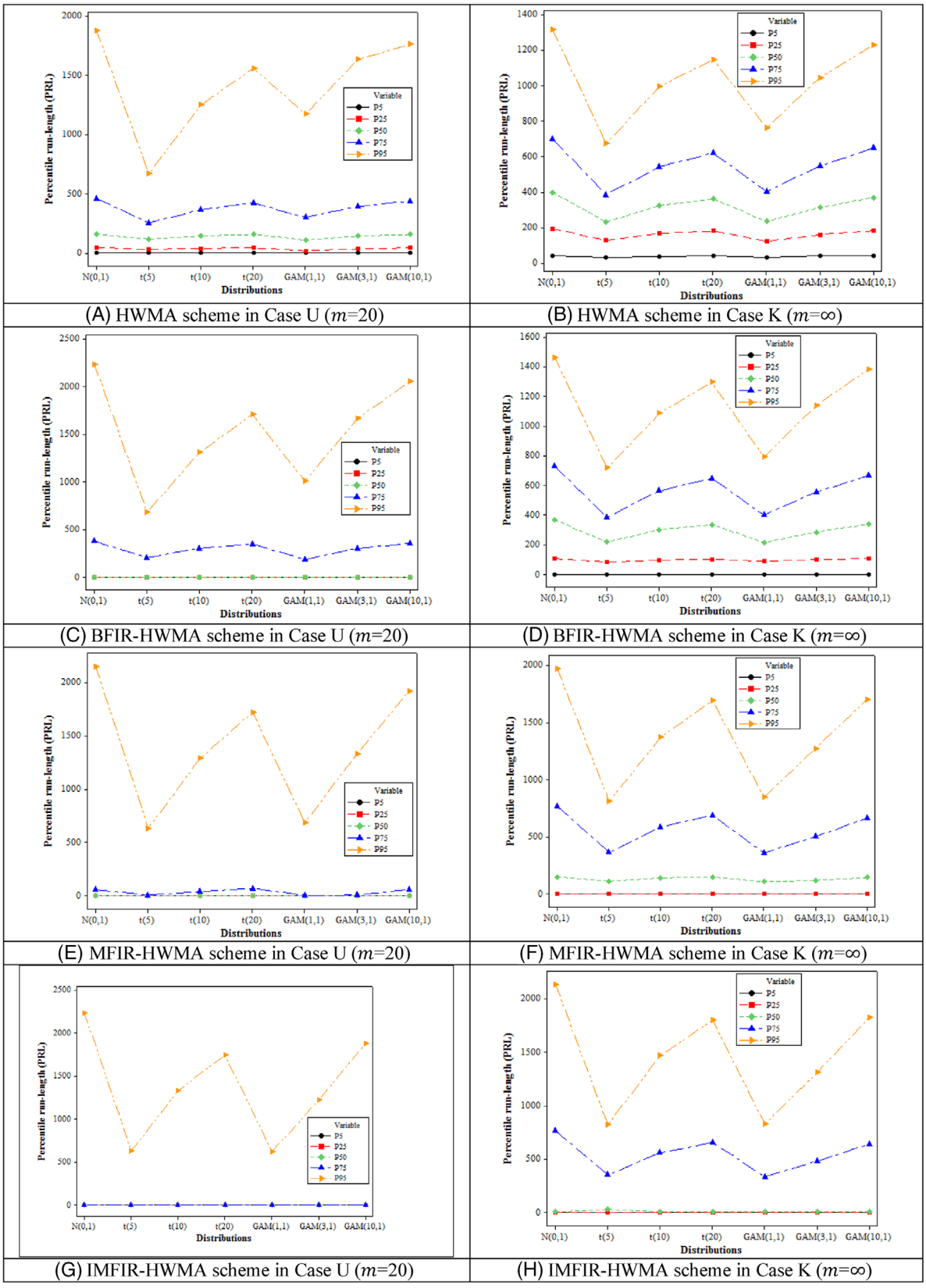

FIGURE 2 Robustness of the HWMA $\bar{X}^*$ scheme with and without FIR features when $n = 5$ and $\lambda = 0.1$ under different continuous probability distribution with a nominal $ARL_0 = 500$

TABLE 2 The *ARL* and *EARL* profiles of the HWMA $\bar{X}^*$ scheme with different FIR features for perfect measurements ($\gamma = 0$ or $C = D = 0$) when $\lambda = 0.1$ and $n = 5$

	Case U (ie, $m = 20$)				Case U (ie, $m = 100$)				Case K (ie, $m = \infty$)			
δ	None	BFIR	MFIR	IMFIR	None	BFIR	MFIR	IMFIR	None	BFIR	MFIR	IMFIR
0.1	308.0	199.5	113.2	87.8	165.4	131.3	91.3	76.1	95.8	85.9	65.9	60.4
0.2	75.2	34.3	16.3	14.2	43.0	33.2	21.7	17.1	34.1	29.1	21.6	17.6
0.3	23.7	12.9	7.4	5.1	20.6	15.1	10.2	7.3	17.9	14.1	10.1	7.6
0.4	13.2	7.3	4.3	2.9	12.6	8.4	5.7	3.9	11.2	7.9	5.6	4.0
0.5	8.8	4.6	2.8	2.0	8.6	5.3	3.6	2.5	7.8	5.0	3.4	2.6
0.6	6.3	3.3	2.1	1.6	6.3	3.7	2.5	1.9	5.9	3.5	2.4	1.9
0.7	4.9	2.5	1.7	1.5	4.9	2.7	1.9	1.6	4.7	2.6	1.8	1.6
0.8	4.0	2.1	1.5	1.3	4.0	2.2	1.6	1.4	3.9	2.1	1.5	1.4
0.9	3.4	1.8	1.4	1.3	3.4	1.9	1.4	1.3	3.3	1.8	1.3	1.3
1.0	2.9	1.6	1.3	1.2	2.9	1.6	1.3	1.2	2.9	1.5	1.2	1.2
$EARL_{(0,1]}$	45.0	27.0	15.2	11.9	27.2	20.5	14.1	11.4	18.7	15.4	11.5	10.0
L^*	3.493	3.569	3.703	3.752	3.330	3.435	3.613	3.667	2.938	3.005	3.166	3.225

TABLE 3 The *SDRL* and *ESDRL* profiles of the HWMA $\bar{X}^*$ scheme with different FIR features for perfect measurements ($\gamma = 0$ or $C = D = 0$) when $\lambda = 0.1$ and $n = 5$

	Case U (ie, $m = 20$)				Case U (ie, $m = 100$)				Case K (ie, $m = \infty$)			
δ	None	BFIR	MFIR	IMFIR	None	BFIR	MFIR	IMFIR	None	BFIR	MFIR	IMFIR
0.1	1105.2	1043.7	969.8	947.7	246.1	242.2	241.9	194.8	68.8	76.0	84.4	86.9
0.2	355.2	215.8	38.4	32.3	37.0	37.7	34.8	31.6	21.7	24.7	26.6	26.1
0.3	33.8	19.3	14.9	12.1	14.4	15.9	15.3	13.4	10.7	12.3	12.9	11.7
0.4	12.3	10.1	8.1	5.9	7.9	8.8	8.4	6.6	6.3	7.3	7.2	5.9
0.5	7.3	6.0	4.7	3.1	5.1	5.5	5.1	3.5	4.2	4.6	4.5	3.2
0.6	4.8	3.9	2.9	1.8	3.6	3.6	3.2	2.0	3.0	3.0	2.8	1.9
0.7	3.5	2.6	1.9	1.1	2.7	2.4	2.1	1.3	2.3	2.2	1.9	1.3
0.8	2.7	1.8	1.4	0.8	2.1	1.8	1.5	0.9	1.8	1.6	1.3	1.0
0.9	2.1	1.4	1.0	0.6	1.8	1.4	1.1	0.7	1.5	1.3	0.9	0.7
1.0	1.7	1.1	0.8	0.5	1.5	1.1	0.8	0.6	1.3	1.0	0.7	0.6
$ESDRL_{(0,1]}$	152.9	130.6	104.4	100.6	32.2	32.0	31.4	25.5	12.2	13.4	14.3	13.9
L^*	3.493	3.569	3.703	3.752	3.330	3.435	3.613	3.667	2.938	3.005	3.166	3.225

Case K—see the pattern depicted by the *ESDRL* values. More importantly, it is observed in Table 3 that there is a higher variability (ie, *SDRL*) when the Phase I sample is small and as m increase, the OOC *SDRL* values decrease for the HWMA scheme with or without the FIRs. Thus, it is highly recommended in Case U to use a relatively higher Phase I sample size. Finally, while the IC *SDRL* of the IMFIR-HWMA scheme is the highest (especially in Case U); however, in the OOC situations, the *SDRL*s are either the smallest or comparatively the same as other competing schemes in Table 3.

3.3.2 | HWMA $\bar{X}^*$ scheme for different FIR features with measurement errors

Next, Table 4 displays the *ARL* and *EARL* profiles of the HWMA $\bar{X}^*$ scheme with "no FIR," BFIR, MFIR, and IMFIR features with a constant variance for single measurements when B =1 and $\gamma \in \{0, 0.5, 0.9\}$. However, Table 5 displays the same for the *SDRL* and *ESDRL* profiles. First, the constant A in Equations (3) to (6) do not have any effect on the *RL* performance; hence, for any value of A, the *ARL* and *EARL* values are the same. Second, as γ increases, the performance of the HWMA $\bar{X}^*$ scheme for each FIR and "no FIR" feature deteriorates in terms of the *ARL*, *SDRL*, *EARL*, and *ESDRL*. That is, for the same input parameters, the *ARL*, *SDRL*, *EARL*, and *ESDRL* values for $\gamma = 0$ in Tables 2 and 3 are lower than those of $\gamma = 0.5$ and 0.9 in Tables 4 and 5. Moreover, in Table 4, the *ARL* and *EARL* values for $\gamma = 0.5$ are lower than those

TABLE 4 The *ARL* and *EARL* profiles of the HWMA $\bar{X}^*$ scheme with different FIR features for a constant measurement system error when $\gamma \in \{0.5, 0.9\}$, $r = 1$, $m = 100$, $\lambda = 0.1$, and $n = 5$

	$\gamma = 0.5$				$\gamma = 0.9$			
Shift	**None**	**BFIR**	**MFIR**	**IMFIR**	**None**	**BFIR**	**MFIR**	**IMFIR**
0.1	199.1	164.4	114.5	98.3	259.2	217.4	168.9	141.4
0.2	53.2	41.3	27.5	21.7	76.9	58.2	38.9	31.8
0.3	25.3	18.6	12.6	9.2	35.1	26.8	18.0	13.7
0.4	15.2	10.5	7.2	5.0	21.0	15.4	10.2	7.4
0.5	10.4	6.6	4.6	3.0	14.2	9.7	6.6	4.5
0.6	7.5	4.6	3.1	2.2	10.4	6.6	4.5	3.0
0.7	5.9	3.4	2.3	1.8	7.9	4.8	3.3	2.3
0.8	4.8	2.7	1.9	1.5	6.4	3.7	2.5	1.9
0.9	4.0	2.2	1.6	1.4	5.3	3.0	2.1	1.7
1.0	3.4	1.9	1.4	1.3	4.5	2.5	1.8	1.5
$\boldsymbol{EARL}_{(0,1]}$	32.9	25.6	17.7	14.5	44.1	34.8	25.7	20.9

TABLE 5 The *ARL* and *EARL* profiles of the HWMA $\bar{X}^*$ scheme with different FIR features for a constant measurement system error when $\gamma \in \{0.5, 0.9\}$, $r = 1$, $m = 100$, $\lambda = 0.1$, and $n = 5$

	$\gamma = 0.5$				$\gamma = 0.9$			
Shift	**None**	**BFIR**	**MFIR**	**IMFIR**	**None**	**BFIR**	**MFIR**	**IMFIR**
0.1	302.4	304.8	291.8	301.0	371.9	381.8	460.3	411.1
0.2	53.9	49.8	44.9	41.4	96.4	78.0	72.3	61.9
0.3	18.1	20.0	18.9	17.0	27.8	29.0	28.0	25.3
0.4	9.8	11.0	10.7	8.8	14.6	16.1	15.5	13.5
0.5	6.4	6.9	6.6	4.7	9.3	10.2	9.8	7.9
0.6	4.4	4.7	4.2	2.7	6.4	7.0	6.6	4.8
0.7	3.3	3.2	2.9	1.8	4.7	4.9	4.5	3.1
0.8	2.6	2.3	2.0	1.2	3.7	3.6	3.3	2.0
0.9	2.1	1.8	1.5	0.9	3.0	2.7	2.4	1.5
1.0	1.8	1.4	1.1	0.7	2.4	2.1	1.8	1.1
$\boldsymbol{ESDRL}_{(0,1]}$	40.5	40.6	38.4	38.0	54.0	53.5	60.5	53.2

of $\gamma = 0.9$; a similar pattern is observed in Table 5 for the *SDRL* and *ESDRL*. Finally and more importantly, it is observed that the relation outlined in Ref. (16) also hold for the HWMA $\bar{X}^*$ scheme with constant measurement system variance in terms of *ARL* and *EARL* metrics.

Table 6 displays the *ARL* and *EARL* profiles of the HWMA $\bar{X}^*$ scheme with "no FIR," BFIR, MFIR, and IMFIR features for a linearly increasing variance when $C = 0$, $B = 1$ and $D \in \{1,2,3\}$. It is observed that for a specific B and C, as D increases, the *ARL* and *EARL* values also increase for the HWMA $\bar{X}^*$ schemes integrated with each FIR feature. Similarly, for a specific B and D, as C increases, the *ARL* and *EARL* values also increase (this not shown to preserve space). For some specific input parameters, the IMFIR-HWMA scheme has the best OOC *ARL* and *EARL* performance than the competitors in Table 6. For instance, when $D = 1$, the *ARL* when $\delta = 0.1$ is equal to 272.9, 238.0, 185.1, and 160.0 for the HWMA, BFIR-HWMA, MFIR-HWMA, and IMFIR-HWMA, respectively. The *SDRL* and *ESDRL* depict a similar pattern as D increases; hence for brevity, this is not shown here.

3.3.3 | HWMA $\bar{X}^*$ scheme for different FIR features with multiple measurements

In Table 7 that when r is increases from 1 to 4 (in parenthesis), the *ARL* and *EARL* values decrease for each HWMA $\bar{X}^*$ schemes with and without FIR features. Although the latter improvement is illustrated for $\gamma = 0.5$, it is important to note that it occurs whenever $\gamma > 0$. Moreover, it is again observed that the relation in Equation (16) also holds for the

TABLE 6 *RL* and *EARL* profiles of the HWMA $\bar{X}^*$ scheme with linearly increasing variance where $D \in \{1, 2, 3\}$ B =1, $C = 0$, λ =0.1, $n = 5$, $r = 1$, and $m = 100$

	None			BFIR			MFIR			IMFIR		
Shift	$D = 1$	$D = 2$	$D = 3$	$D = 1$	$D = 2$	$D = 3$	$D = 1$	$D = 2$	$D = 3$	$D = 1$	$D = 2$	$D = 3$
0.1	272.9	329.0	366.7	238.0	296.3	348.0	185.1	237.7	293.1	160.0	217.8	256.7
0.2	85.7	127.8	164.6	65.5	100.8	131.0	44.1	65.9	90.8	35.7	55.5	76.2
0.3	38.6	57.7	75.7	29.3	43.6	57.4	19.6	29.4	38.3	15.4	23.4	31.2
0.4	23.0	33.1	43.1	16.8	25.0	33.2	11.4	16.9	22.2	8.2	12.9	17.4
0.5	15.4	22.3	28.5	10.7	16.3	21.4	7.3	10.8	14.6	5.1	7.8	11.1
0.6	11.3	16.0	20.8	7.4	11.3	14.9	5.0	7.5	10.1	3.4	5.2	7.4
0.7	8.7	12.3	15.9	5.3	8.3	11.0	3.6	5.6	7.6	2.6	3.8	5.2
0.8	6.9	9.8	12.5	4.1	6.2	8.4	2.8	4.2	5.7	2.1	2.8	3.8
0.9	5.8	8.0	10.3	3.3	4.9	6.5	2.3	3.3	4.5	1.8	2.4	3.0
1.0	4.9	6.7	8.6	2.7	3.9	5.3	1.9	2.7	3.5	1.6	2.0	2.5
$\boldsymbol{EARL}_{(0,1]}$	47.3	62.3	74.6	38.3	51.7	63.7	28.3	38.4	49.0	23.6	33.3	41.4

TABLE 7 The *ARL* and *EARL* profiles of the HWMA $\bar{X}^*$ scheme with a constant variance where $\gamma = 0.5$ when $m = 100$, $B = 1$, $\lambda = 0.1$, $n = 5$, and $r = 1$ (with $r = 4$ in parenthesis)

Shift	**None**	**BFIR**	**MFIR**	**IMFIR**
0.1	199.1 (174.0)	164.4 (138.1)	114.5 (97.1)	98.3 (79.9)
0.2	53.2 (45.5)	41.3 (35.4)	27.5 (23.2)	21.7 (18.6)
0.3	25.3 (21.7)	18.6 (15.9)	12.6 (11.0)	9.2 (7.8)
0.4	15.2 (13.1)	10.5 (8.9)	7.2 (6.0)	5.0 (4.1)
0.5	10.4 (9.0)	6.6 (5.6)	4.6 (3.9)	3.0 (2.6)
0.6	7.5 (6.6)	4.6 (3.9)	3.1 (2.7)	2.2 (1.9)
0.7	5.9 (5.2)	3.4 (2.9)	2.3 (2.0)	1.8 (1.6)
0.8	4.8 (4.2)	2.7 (2.3)	1.9 (1.7)	1.5 (1.4)
0.9	4.0 (3.5)	2.2 (2.0)	1.6 (1.5)	1.4 (1.3)
1.0	3.4 (3.1)	1.9 (1.7)	1.4 (1.3)	1.3 (1.2)
$\boldsymbol{EARL}_{(0,1]}$	32.9 (28.6)	25.6 (21.7)	17.7 (15.0)	14.5 (12.1)

different HWMA schemes with and without FIR features for any given r value (this is, in part, further illustrated in the next subsection). In Table 8, it is shown that the corresponding OOC *SDRL* also decrease for each HWMA scheme with and without FIR features when more measurements per item are taken.

Similarly (although not shown here to preserve space, but part of it is illustrated in the next subsection), the HWMA $\bar{X}^*$ scheme with linearly increasing variance has the same relation shown in Equation (16) for the magnitude of the *ARL* and *EARL* in Cases K and U when multiple measurements are taken and the *SDRL*s decrease when r increases.

Given that Tables 2–8 indicate that the IMFIR-HWMA $\bar{X}^*$ scheme has the best OOC *ARL* performance than the other considered HWMA $\bar{X}^*$ scheme with and without FIR features; hence, in the next subsection, the IMFIR-HWMA $\bar{X}^*$ scheme is studied in more details.

3.3.4 | IMFIR-HWMA $\bar{X}^*$ scheme

In this subsection, the effect of varying the design parameters B, r, and λ are illustrated graphically for the IMFIR-HWMA $\bar{X}^*$ scheme when the measurement system has a constant and linearly increasing variance using the *ARL* and *SDRL*. First, increasing either B or r, it is observed in Figures 3 and 4 that the OOC *ARL* and *SDRL* values decrease indicating an improving performance of the IMFIR-HWMA $\bar{X}^*$ scheme. Second, for small shift values, the *ARL* are smaller than the corresponding *SDRL*; however, as the shift increases, the *SDRL*s tend to be smaller than the corresponding *ARL*s. Third, as the smoothing parameter λ increases, it is observed that at each shift value the *ARL*s and *SDRL*s have higher magnitudes

TABLE 8 The *SDRL* and *ESDRL* profiles of the HWMA $\bar{X}^*$ scheme with a constant variance where $\gamma = 0.5$ when $m = 100$, $B = 1$, $\lambda = 0.1$, $n = 5$, and $r = 1$ (with $r = 4$ in parenthesis)

Shift	None	BFIR	MFIR	IMFIR
0.1	302.4 (261.2)	304.8 (247.8)	291.8 (252.2)	301.0 (203.4)
0.2	53.9 (41.6)	49.8 (40.8)	44.9 (37.2)	41.4 (34.3)
0.3	18.1 (15.1)	20.0 (16.8)	18.9 (16.4)	17.0 (14.1)
0.4	9.8 (8.3)	11.0 (9.4)	10.7 (8.9)	8.8 (7.0)
0.5	6.4 (5.4)	6.9 (5.8)	6.6 (5.4)	4.7 (3.8)
0.6	4.4 (3.8)	4.7 (3.8)	4.2 (3.5)	2.7 (2.2)
0.7	3.3 (2.8)	3.2 (2.6)	2.9 (2.3)	1.8 (1.4)
0.8	2.6 (2.3)	2.3 (1.9)	2.0 (1.6)	1.2 (1.0)
0.9	2.1 (1.9)	1.8 (1.5)	1.5 (1.2)	0.9 (0.8)
1.0	1.8 (1.6)	1.4 (1.2)	1.1 (0.9)	0.7 (0.6)
$\boldsymbol{EARL}_{(0,1]}$	40.5 (34.4)	40.6 (33.1)	38.4 (32.9)	38.0 (26.9)

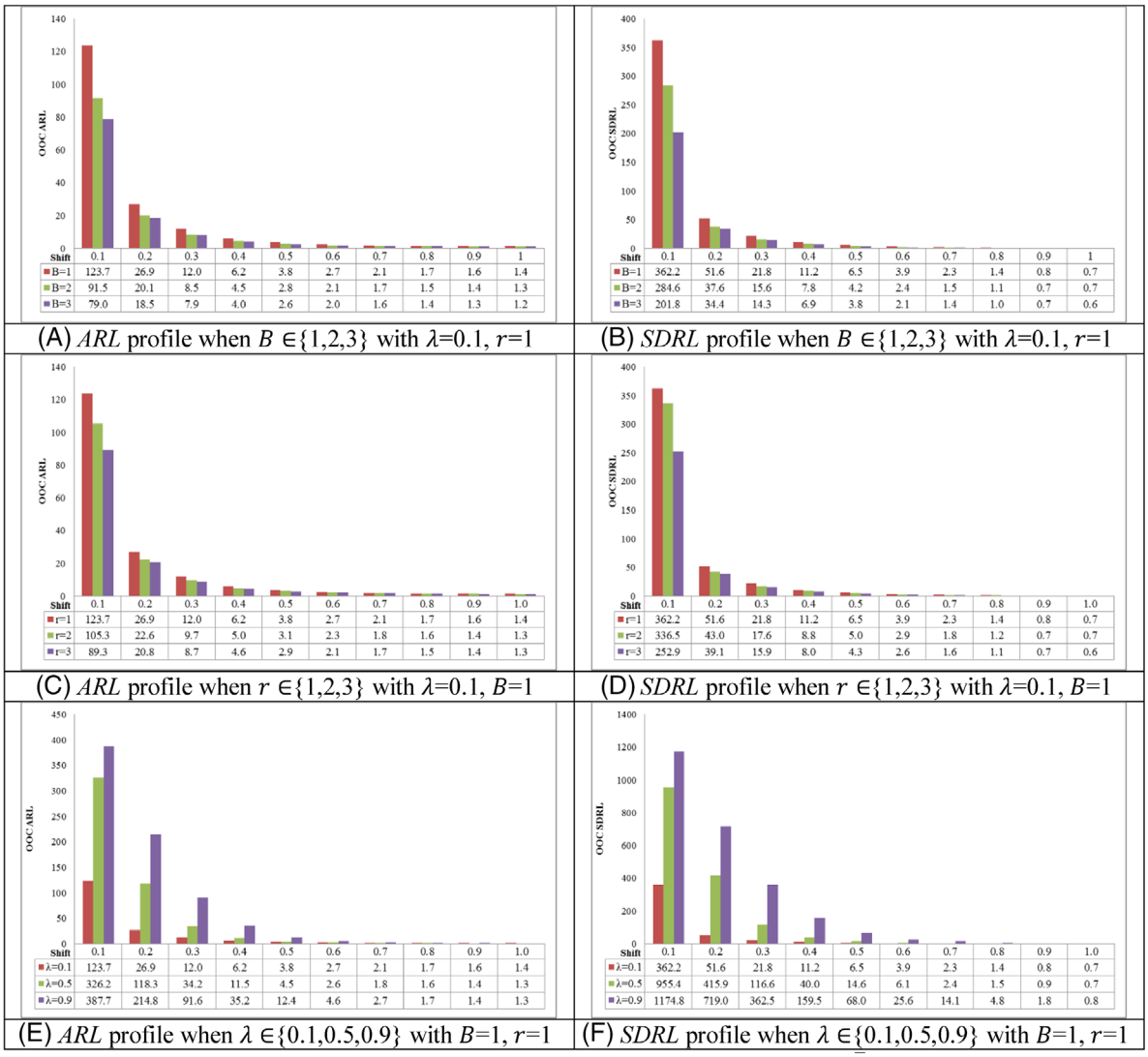

FIGURE 3 Effect of B, r, and λ on the Phase II performance of the IMFIR-HWMA $\bar{X}^*$ scheme in terms of *ARL* and *SDRL* when the measurement system is under the effect of a constant variance with $\gamma = 0.75$, $m = 100$, $n = 5$, and $ARL_0 = 500$

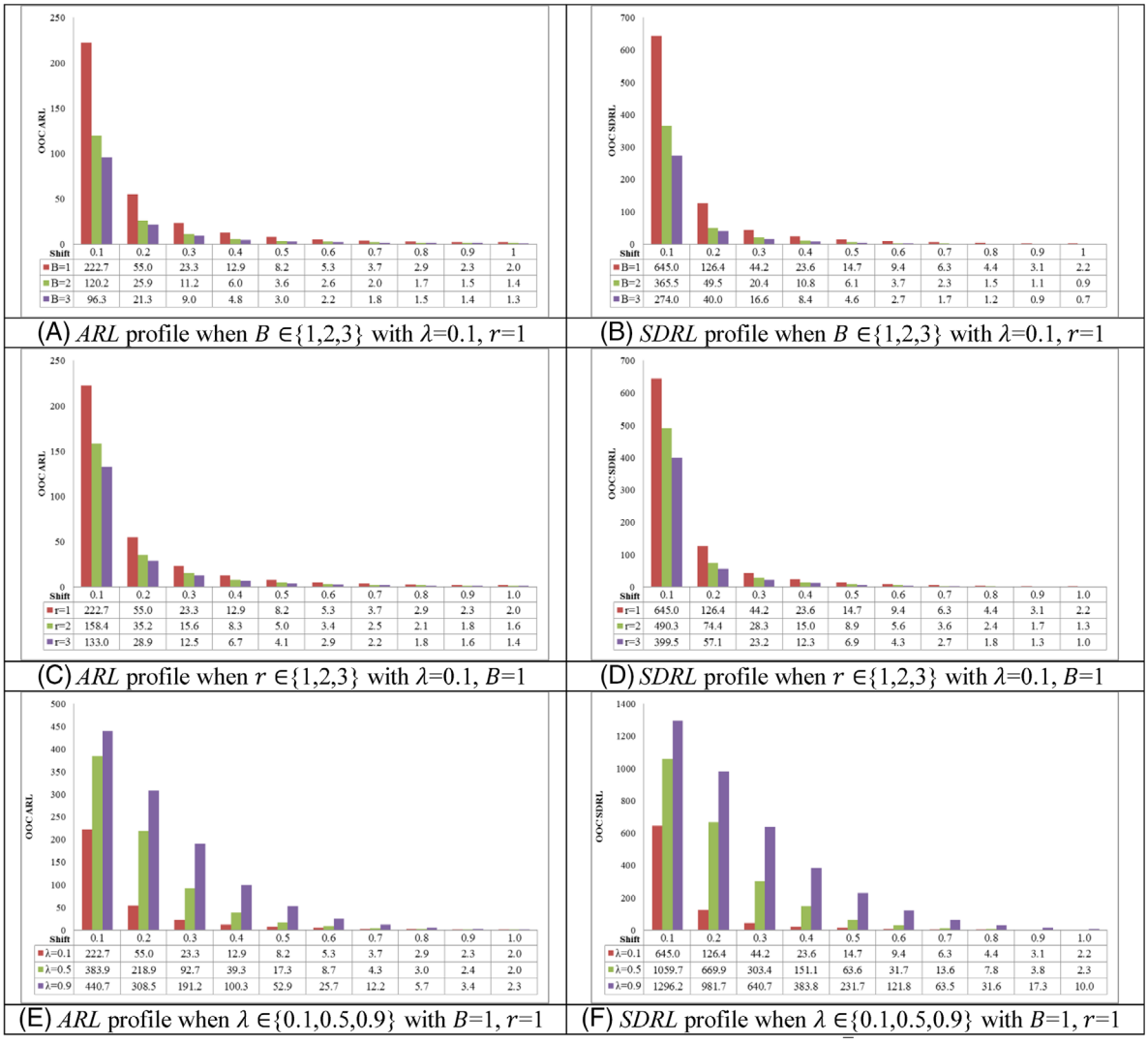

FIGURE 4 Effect of B, r, and λ on the Phase II performance of the IMFIR-HWMA $\bar{X}^*$ scheme in terms of *ARL* and *SDRL* when the measurement system is under the effect of a linearly increasing variance with $C = D = 1$, $m = 100$, $n = 5$, and $ARL_0 = 500$

as compared to the corresponding values with smaller λ values. For the IC *ARL* to be approximately equal to 500 when $m = 100$ in Figures 3 and 4, then the pair of design parameters, that is, (λ, L^*), are given by (0.1, 3.6674), (0.5, 3.6163), and (0.9, 3.6515). It is worth mentioning that similar patterns are also observed for the HWMA schemes (for constant and linearly increasing variance scenarios) with BFIR and MFIR features; however, in each instance, the HWMA scheme with IMFIR feature yields the best OOC *ARL* performance than the latter competing features.

4 | ILLUSTRATIVE EXAMPLE

In order to illustrate the implementation of the HWMA and IMFIR-HWMA $\bar{X}^*$ schemes with measurement error under constant variance in Case U, the data from Tran et al[42] are used (see Table 9). The data are based on a real-life application from the volume of milk within a bottle where the quality characteristic $X^*_{t,i,j}$ is the volume (in milliliters) of milk. In this example, using $m = 20$ Phase I samples, the IC mean and the IC standard deviation are $\hat{\mu}_0 = 500.023\ ml$ and $\hat{\sigma}_0 = 0.9616$ mL, respectively. The data contain one set of 20 subgroups each of size 5 (ie, $n = 5$, $r = 1$ and $t = 1, \ldots, 20$). As in Tran et al,[42] the parameters of the covariate model are $\gamma = 0.28$, $A = 0$ and $B = 1$. For a nominal ARL_0 value of 500 and $\lambda = 0.1$, it is found that $L^* = 3.493$ and 3.752 for the HWMA and IMFIR-HWMA $\bar{X}^*$ schemes, respectively. The plotting statistics and control limits of the HWMA and IMFIR-HWMA $\bar{X}^*$ schemes when $\lambda = 0.1$ are shown in Figure 5(A). When

TABLE 9 Dataset on the volume of milk in each bottle during a filling process (in milliliters)

t	$X^*_{t,1,1}$	$X^*_{t,2,1}$	$X^*_{t,3,1}$	$X^*_{t,4,1}$	$X^*_{t,5,1}$
1	500.46	498.99	500.22	500.41	498.96
2	500.06	500.20	499.31	501.07	499.57
3	498.82	501.55	499.48	499.20	501.56
4	502.64	502.86	500.06	499.08	500.72
5	500.06	500.03	500.09	498.88	497.64
6	500.50	499.54	499.02	498.09	499.87
7	498.89	500.20	501.10	502.01	500.99
8	500.37	499.28	500.15	500.87	500.88
9	499.81	500.62	500.68	500.67	500.00
10	499.79	499.87	500.98	499.12	500.79
11	502.39	500.61	501.29	500.32	500.74
12	500.35	500.57	501.80	502.03	499.56
13	499.49	501.09	499.53	499.82	499.90
14	500.96	500.87	502.71	500.70	499.71
15	500.85	499.88	500.58	501.62	501.04
16	500.48	502.82	501.00	501.78	501.73
17	502.01	501.18	500.67	501.31	499.98
18	501.36	501.11	500.27	501.12	501.98
19	499.92	500.13	501.46	502.29	502.78
20	502.19	500.30	499.03	500.17	502.19

$\lambda = 0.9$, it is found that $L^* = 3.227$ and 3.548 for the HWMA and IMFIR-HWMA $\bar{X}^*$ schemes, respectively (see Figure 5B). From Figure 5, it can be seen that the control limits of the IMFIR-HWMA $\bar{X}^*$ scheme shrunk considerably for $t < 15$, as compared to the standard one. Thus, for a small smoothing parameter, that is, $\lambda = 0.1$, there are no major start-up problems; both schemes give a signal on the 16th subgroup. However, for a large smoothing parameter, that is, $\lambda = 0.9$, the standard HWMA scheme signals on the 16th subgroup; while the one with the IMFIR feature gives a signal much sooner, that is, on the 4th subgroup. Therefore, the IMFIR-HWMA $\bar{X}^*$scheme is found to be superior to the standard HWMA $\bar{X}^*$ scheme with no FIR feature.

5 | CONCLUSION

In this paper, different FIR features are incorporated to the design of the HWMA $\bar{X}^*$ scheme in order to improve its sensitivity in detecting shifts in the mean during start-up period for processes with and without measurement errors. Moreover, a comparative study of the HWMA $\bar{X}^*$ schemes with and without measurement errors reveal that the IMFIR feature outperforms the "no FIR" feature as well as the BFIR and MFIR features. This study has also shown that the simultaneous use of the IMFIR feature and multiple measurements with $r \leq 4$, yields a significant improvement on the performance of the HWMA $\bar{X}^*$ scheme during start-up period. In addition, a higher value for the coefficient B in the covariate error model yields a better performance in the proposed monitoring scheme. Practitioners in the industries are recommended to use the IMFIR-HWMA scheme in real-life applications in order to efficiently detect start-up problems. Finally, relatively high Phase I sample sizes are recommended for a better Phase II HWMA $\bar{X}^*$ schemes' performance.

The scope of current study covers the processes in which characteristics follow a normal distribution and observations are assumed to be i.i.d. Therefore, it is recommended to study the corresponding performance for nonnormal distributions and simultaneously taking autocorrelation and measurement errors into account. Moreover, the IMFIR feature need to be implemented for different time-varying memory-type schemes to monitor variability, joint mean and variability parameter(s) for better detection at start-up period. Also, in an effort to improve detection ability at start-up for the HWMA scheme to monitor variability,[43] we intend to incorporate the FIR features discussed here in the latter scheme. Finally, the

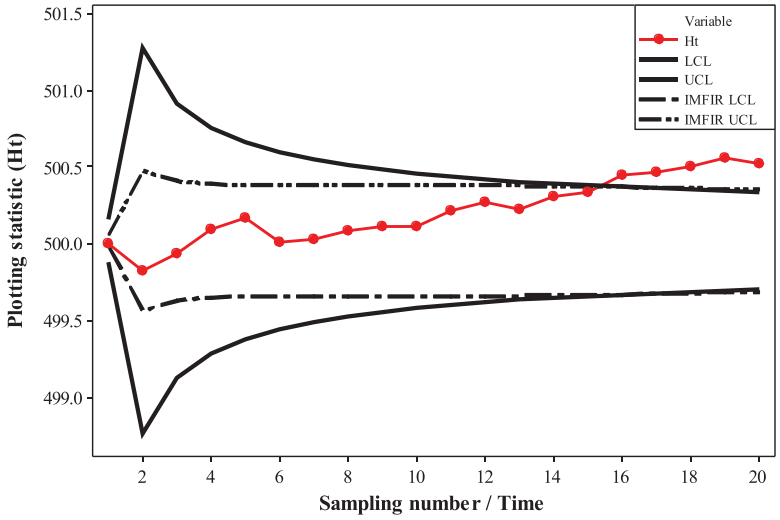

(A) $\lambda = 0.1$

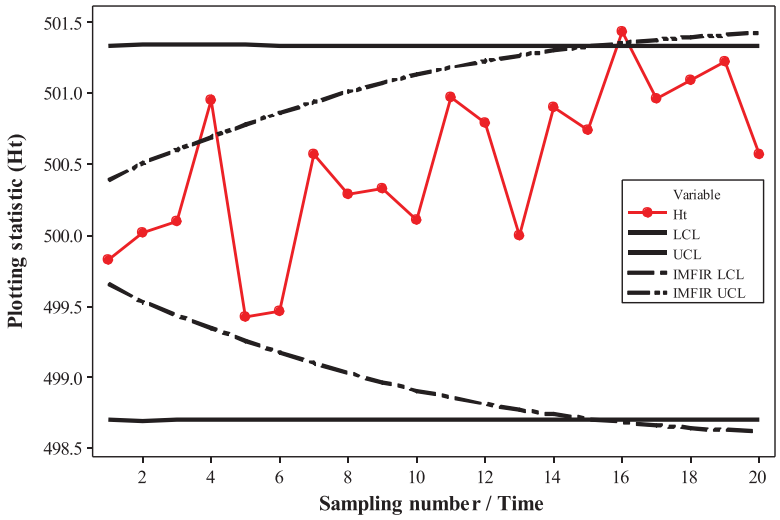

(B) $\lambda = 0.9$

FIGURE 5 Illustration example of the standard "no FIR" HWMA and IMFIR-HWMA $\bar{X}^*$ schemes in Case U using the filling process of milk bottles

FIR features discussed here can also be incorporated on the double and hybrid HWMA schemes, which are discussed in Alevizakos et al.[44]

ACKNOWLEDGMENTS

The authors would like to thank the reviewers and the editorial team for taking their valuable time to evaluate our manuscript.

DATA AVAILABILITY STATEMENT

The data used in the application example is provided within the paper and the SAS® v.9.4 programs used here can be requested from the authors.

ORCID

Saddam Akber Abbasi https://orcid.org/0000-0003-1843-8863
Jean-Claude Malela-Majika https://orcid.org/0000-0001-7236-7678
Muhammad Aslam https://orcid.org/0000-0003-0644-1950
Sandile Charles Shongwe https://orcid.org/0000-0003-2243-8196

REFERENCES

1. Montgomery DC. *Statistical Quality Control: A Modern Introduction*. 7th ed. New Jersey, Hoboken: John Wiley & Sons; 2013.
2. Chakraborti S, Graham MA. *Nonparametric Statistical Process Control*. New York: Wiley; 2019.
3. Aslam M, Saghir A, Ahmad L. *Introduction to Statistical Process Control*. New York: Wiley; 2020.
4. Does RJMM, Goedhart R, Woodall WH. On the design of control charts with guaranteed conditional performance under estimated parameters. *Qual Reliab Eng Int*. 2020;36(8):2610-2620.
5. Page ES. Continuous inspection schemes. *Biometrika*. 1959;41(1-2):100-115.
6. Roberts SW. Control chart tests based on geometric moving averages. *Technometrics*. 1954;1(3):239-250.
7. Sheu S-H, Lin T-C. The generally weighted moving average control chart for detecting small shifts in the process mean. *Qual Eng*. 2003;16(2):209-231.
8. Abbas N. Homogeneously weighted moving average control chart with an application in substrate manufacturing process. *Comp Ind Eng*. 2018;120:460-470.
9. Adegoke NA, Smith ANH, Anderson MJ, Sanusi RA, Pawley MDM. Efficient homogeneously weighted moving average chart for monitoring process mean using an auxiliary variable. *IEEE Access*. 2019;7:94021-94032.
10. Adegoke NA, Abbasi SA, Smith ANH, Anderson MJ, Pawley MDM. A multivariate homogeneously weighted moving average control chart. *IEEE Access*. 2019;7:9586-9597.
11. Abbas N, Riaz M, Ahmad S, Abid M, Zaman B. On the efficient monitoring of multivariate processes with unknown parameters. *Mathematics*. 2020;8(5):823.
12. Nawaz T, Han D. Monitoring the process location by using new ranked set sampling-based memory control charts. *Qual Tech Quant Manag*. 2020;17(3):255-284.
13. Raza M, Nawaz T, Han D. On designing distribution-free homogeneously weighted moving average control charts. *J Test Eval*. 2020;48(4):3154-3171.
14. Adeoti OA, Koleoso SO. A hybrid homogeneously weighted moving average control chart for process monitoring. *Qual Reliab Eng Int*. 2020;36(6):2170-2186.
15. Abid M, Shabbir A, Nazir HZ, Sherwani RAK, Riaz M. A double homogeneously weighted moving average control chart for monitoring of the process mean. *Qual Reliab Eng Int*. 2020;36(5):1513-1527.
16. Abid M, Mei S, Nazir HZ, Riaz M, Hussain S. A mixed HWMA-CUSUM mean chart with an application to manufacturing process. *Qual Reliab Eng Int*. 2020;37(2):618-631.
17. Dawod A, Adegoke NA, Abbasi SA. Efficient linear profile schemes for monitoring bivariate correlated processes with applications in the pharmaceutical industry. *Chem Intell Lab Syst*. 2020;206:104137.
18. Thanwane M, Malela-Majika J-C, Castagliola P, Shongwe SC. The effect of measurement errors on the performance of the homogeneously weighted moving average X monitoring scheme. *Trans Inst Meas and Contr*. 2020;43(3):728-745.
19. Thanwane M, Malela-Majika J-C, Castagliola P, Shongwe SC. The effect of measurement errors on the performance of the homogeneously weighted moving average X monitoring scheme with estimated parameters. *J Stat Comput Simul*. 2020:1-25. https://doi.org/10.1080/00949655.2020.1850728.
20. Thanwane M, Shongwe SC, Malela-Majika J-C, Aslam M. Parameter estimation effect of the homogeneously weighted moving average chart to monitor the mean of autocorrelated observations with measurement errors. *IEEE Access*. 2020;8:221352-221366.
21. Steiner SH. EWMA control charts with time-varying control limits and fast initial response. *J Qual Tech*. 1999;31(3):75-86.
22. Knoth S. Fast initial response features for EWMA control charts. *Stat Papers*. 2005;46(1):47-64.
23. Chiu W-C. Generally weighted moving average control charts for fast initial response features. *J Appl Stat*. 2009;36(3):255-275.
24. Haq A, Brown J, Moltchanova E. Improved fast initial response features for exponentially weighted moving average and cumulative sum control charts. *Qual Reliab Eng Int*. 2014;30(5):697-710.
25. Letshedi TI, Malela-Majika J-C, Castagliola P, Shongwe SC. Distribution-free triple EWMA control chart for monitoring the process location using the Wilcoxon rank-sum statistic with fast initial response feature. *Qual Reliab Eng Int*. 2020. https://doi.org/10.1002/qre.2842.
26. Maleki MR, Amiri A, Castagliola P. Measurement errors in statistical process monitoring: a literature review. *Comp Ind Eng*. 2017;103:316-329.
27. Linna KW, Woodall WH. Effect of measurement error on Shewhart control charts. *J Qual Tech*. 2001;33(2):213-222.
28. Maravelakis P, Panaretos J, Psarakis S. EWMA chart and measurement error. *J Appl Stat*. 2004;31(4):445-455.
29. Maravelakis P. Measurement error on the CUSUM control chart. *J Appl Stat*. 2012;39(2):323-336.
30. Riaz A, Noor-ul-Amin M, Shehzad MA, Ismail M. Auxiliary information based mixed EWMA-CUSUM mean control chart with measurement error. *Iran J Sc Tech, Transact A: Sc*. 2019;43(6):2937-2949.
31. Sabahno H, Amiri A, Castagliola P. Optimal performance of the variable sample sizes Hotelling's T2 control chart in the presence of measurement errors. *Qual Tech Quant Manag*. 2019;16(5):588-612.
32. Sabahno H, Castagliola P, Amiri A. A variable parameters multivariate control chart for simultaneous monitoring of the process mean and variability with measurement errors. *Qual Reliab Eng Int*. 2020;36(4):1161-1196.
33. Zaidi FS, Castagliola P, Tran KP, Khoo MBC. Performance of the Hotelling's T^2 control chart for compositional data in the presence of measurement errors. *J Appl Stat*. 2019;46(14):2583-2602.
34. Zaidi FS, Castagliola P, Tran KP, Khoo MBC. Performance of the MEWMA-CoDa control chart in the presence of measurement errors. *Qual Reliab Eng Int*. 2020;36(7):2411-2440.

35. Nguyen HD, Tran KP, Tran KD. The effect of measurement errors on the performance of the exponentially weighted moving average control charts for the ratio of two normally distributed variables. *European J Oper Res*. 2020;293:203-218. https://doi.org/10.1016/j.ejor.2020.11.042.
36. Noor-ul-Amin M, Javaid A, Hanif M, Dogu E. Performance of maximum EWMA control chart in the presence of measurement error using auxiliary information. *Comm Stat Simul Comp*. 2020:1-25. https://doi.org/10.1080/03610918.2020.1772301.
37. Jensen WA, Jones-Farmer LA, Champ CW, Woodall WH. Effects of parameter estimation on control chart properties: a literature review. *J Qual Tech*. 2006;38(4):349-364.
38. Psarakis S, Vyniou A, Castagliola P. Some recent developments on the effects of parameter estimation on control charts. *Qual Reliab Eng Int*. 2013;30(8):1113-1129.
39. Leong RNF, Co FF, Mojica VJC, Tan DSY. An exponentially weighted moving average control chart for zero-truncated Poisson processes: a design and analytic framework with fast initial response feature. *Philippine Stat*. 2017;66(1):21-40.
40. Tran KP, Castagliola P, Balakrishnan N. On the performance of Shewhart median chart in the presence of measurement errors. *Qual Reliab Eng Int*. 2017;33(5):1019-1029.
41. Shongwe SC, Malela-Majika J-C, Castagliola P. A combined mixed-s-skip sampling strategy to reduce the effect of autocorrelation on the X scheme with and without measurement errors. *J Appl Stat*. 2020:1-26. https://doi.org/10.1080/02664763.2020.1759033.
42. Tran PH, Tran KP, Rakitzis A. A synthetic median control chart for monitoring the process mean with measurement errors. *Qual Reliab Eng Int*. 2020;35(4):1100-1116.
43. Riaz M, Abbasi SA, Abid M, Hamzat AK. A new HWMA dispersion control chart with an application to wind farm data. *Mathematics*. 2020;8(12):2136.
44. Alevizakos V, Chatterjee K, Koukouvinos C. The extended homogeneously weighted moving average control chart. *Qual Reliab Eng Int*. 2021. https://doi.org/10.1002/qre.2849.

AUTHOR BIOGRAPHIES

Maonatlala Thanwane obtained his diploma in compilation of Official Statistics from Eastern Africa Statistical Training Centre in Tanzania (known as EASTC). Also a graduate from the University of South Africa with BSc (Honors) in Statistics and he is currently pursuing his MSc degree in Statistics at the University of South Africa and works at Statistics South Africa (StatsSA) as a data analyst (Survey Statistician).

Saddam Akber Abbasi currently works as an associate professor in Department of Mathematics, Statistics and Physics at Qatar University, Doha, Qatar. He received his PhD in statistics from The University of Auckland, New Zealand in 2013. Before joining Qatar University, Dr Abbasi served as an assistant professor in King Fahd University of Petroleum and Minerals, Dhahran, Saudi Arabia, for 3 years. His research interests include SPC, time-series analysis, profile monitoring, and nonparametric statistics.

Jean-Claude Malela-Majika is a senior lecturer at University of Pretoria's Department of Statistics. He obtained his BSc (honors) degree in mathematical statistics from the High Institute of Statistics from DR Congo, Honours and master's degrees in statistics from University of Pretoria and a PhD in statistics from the University of South Africa. He is a member of the South African Statistical Association, the International Statistical Institute (ISI), and the Institute of Certificated and Chartered Statisticians of South Africa (ICCSSA). His principal research interests include statistical process control/quality control, and statistical inference.

Dr Muhammad Aslam did his MSc (2004) and MPhil (2006) in statistics from GC University Lahore, and PhD in statistics (2010) from National College of Business Administration & Economics Lahore. Currently, he is working as a full professor of Statistics in the Department of Statistics, King Abdul-Aziz University, Jeddah, Saudi Arabia. He has published more than 400 research articles and chapters in national and international well-reputed journals and chapter-contributed books. He is the member of the editorial board of *Electronic Journal of Applied Statistical Analysis*, *Neutrosophic Sets and Systems*, *Pakistan Journal of Commence*, and *Social Sciences and International Journal of Neutrosophic Science*. His research interest includes industrial statistics, neutrosophic inferential statistics, neutrosophic statistics, neutrosophic quality control, neutrosophic applied statistics, and classical applied Statistics.

Sandile Charles Shongwe currently does research at the Department of Statistics at University of South Africa toward PhD. He graduated from University of Pretoria with BSc, BSc (honors), MSc in applied and mathematical statistics. His

current research interest includes the use of statistical process monitoring for autocorrelated data with measurement errors, analysis of big data, and support vector machines.